UHV/CVD and related growth techniques for Si and other materials

D.W. Greve
Department of Electrical and Computer Engineering
Carnegie Mellon University
Pittsburgh, PA 15213
http://www.ece.cmu.edu/~dwg

Abstract

This article discusses the growth of silicon and related materials using ultra-high vacuum chemical vapor deposition (UHV/CVD). This growth technique is well suited for deposition of strained epitaxial layers and also layers with metastable concentrations of impurities such as boron and carbon. In UHV/CVD, growth kinetics and the incorporation of various atoms other than silicon are determined by decomposition of the molecular reactants on the wafer surface. Growth rates, incorporation of dopants and alloy atoms, and various measures of the material quality are discussed. The common features shared with other CVD growth techniques are noted, and the differences are summarized.

Description of UHV/CVD and Motivation

Ultra-high vacuum chemical vapor deposition (UHV/CVD) has been used to describe a variety of growth techniques which have been used for epitaxial layer growth of silicon and related materials. The objectives of most researchers has been the growth of silicon and related materials such as Ge_xSi_{1-x} and $Ge_xSi_{1-x-y}C_y$ as uniformly strained epitaxial layers. One implementation that is of particular commercial interest is the multi-wafer UHV/CVD technique which was first reported [1] and later patented [2] by Meyerson. Notable characteristics of the multi-wafer UHV/CVD technique are the absence of both hydrodynamic boundary-layer effects and gas-phase chemical reactions. This is a consequence of the low total pressure during growth (near 10^{-3} Torr); at such low pressures the molecular mean free path is of the order of the chamber dimensions. Since collisions between molecules are infrequent gas phase reactions are unlikely. Also, a hydrodynamic boundary layer cannot form because transport is by molecular flow. As a result, the growth rate is determined by surface decomposition of the reactant molecules.

Similar, surface-reaction dominated conditions may prevail in other growth systems, depending upon the operating temperature, pressure, and gas residence time. Consequently, this article will discuss not only multi-wafer UHV/CVD results but also those obtained with other techniques.

Figure 1 shows a schematic diagram of a multi-wafer UHV/CVD system. Wafers are arranged on a wafer boat with relatively small inter-wafer spacing (typically a small fraction of the wafer diameter). The wafer boat is positioned in a quartz tube which is heated by a multizone furnace. Gases are introduced at one end and pumped from the other end using UHV-capable throughput pumps (typically a turbopump or a compound turbopump). A load lock is used so that low partial pressures of important contaminants such as hydrocarbons, water vapor, and oxygen can be maintained. This is of crucial importance in low-temperature growth because important contaminants cannot be readily desorbed at the growth temperature. The reactants used are always hydrides (silane, SiH_4; germane, GeH_4; diborane, B_2H_6; methylsilane, SiH_3CH_3; and possibly phosphine, PH_3), diluted in hydrogen or helium to obtain convenient flow rates. The chlorine-containing reactants commonly used in conventional silicon epitaxy are avoided because chlorine tends to persist in the growth system, while the dihydrides used in GSMBE have higher sticking coefficients, which are actually undesirable in multiwafer UHV/CVD since they lead to degraded uniformity as discussed below. Typical growth temperatures are between 500 and 600 °C and the total pressure during growth is generally about 10^{-3} Torr.

Many other researchers have used single-wafer UHV/CVD systems. Typically these are cold-wall systems and use lamp heating [3-6]. Such a system offers more flexibility in the choice of reactants (in particular dichlorosilane (SiH_2Cl_2), is sometimes used). Access for instrumentation, especially optical instrumentation [3], is also easier. One liability of such a system is the wafer throughput compared to a multi-wafer system operating under the same conditions.

Both types of systems can achieve the low contaminant partial pressures required for low-temperature growth. Growth at low temperatures is desired to minimize dopant diffusion. In alloy semiconductors, low growth temperature also limits the formation of misfit dislocations and the rate of surface migration which can lead to undulated layers.

Growth Initiation in UHV/CVD

A major requirement in advanced epitaxial layer growth is the minization of thermal budget, including steps necessary for surface cleaning prior to initiation of epitaxial layer growth. Two different techniques have been used to obtain a contaminant-free silicon surface for UHV/CVD epitaxy. Meyerson [7] describes the preparation of a hydrogen-terminated surface by dipping wafers in dilute hydrofluroric acid with no following rinse (known as an *HF-last* clean). This results in a hydrogen-terminated surface, that is, a surface with virtually all dangling bonds terminated by hydrogen. Such a surface does not react significantly with oxygen or water vapor under ambient conditions. Hydrogen-terminated wafers are loaded into the furnace and flow of reactant gases is initiated before significant desorption of hydrogen can occur. With this approach the wafer is never exposed to any temperature greater than the epitaxial growth temperature.

Alternatively, any oxygen remaining on the wafer surface can be desorbed thermally. Desorption of oxygen in the form of silicon monoxide (SiO) competes with the reactive adsorption of oxygen from water vapor and oxygen in the ambient. Oxygen can be desorbed from the surface at temperatures of 800 °C or slightly lower, and a clean surface will be obtained if the partial pressures of oxygen and water vapor are low enough. Partial pressures must also be low enough to prevent excessive adsorption of oxygen while cooling to the growth temperature.

Oxygen and water vapor partial pressures must correspond to UHV conditions in order to (1) limit the incorporation of oxygen in the epitaxial layer during growth; and (2) to prevent the formation of an oxygen "spike" at the original growth interface, which in extreme cases can cause loss of epitaxial order. Figure 2 shows the maximum allowable partial pressures as a function of temperature along with an estimated time constant for the desorption of oxygen.

Hydrogen termination requires relatively exacting wet chemical processing and also careful control over the introduction of the wafers into the system. Loading is best done just after completion of the wafer clean. After introduction into the load lock typically the wafers are outgassed at moderate temperatures (high enough to desorb physisorbed water and hydrocarbons, but not high enough to desorb surface hydrogen. Timing of the start of deposition is also important, as it is desirable to start the reactive gas flow before a significant amount of hydrogen is desorbed. When performed well, the HF-last clean is capable of excellent results and leads to the lowest possible thermal budget. A final issue with the HF-last clean is the removal of dilute-HF droplets from the wafer surface. This can be problematical for partly silicon-dioxide covered surfaces and may thus require

special fixturing.

The thermal clean places less severe demands on the wet processing, but more stringent demands of the deposition system. The wafers must be cooled rapidly enough after thermal cleaning to prevent significant oxygen adsorption (from residual water vapor) on the wafer surface. This requires moderately rapid cooling and low water vapor pressures. It is worth noting that present users of UHV/CVD in production appear to favor the HF-last clean.

Mechanism of growth and growth rates from silane

As noted earlier, silane is the preferred silicon-containing reactant. We discuss here growth on the (100) surface only; there are some detailed differences on the less-commonly used (111) surface although the general picture is similar. Due to the absence of boundary layer effects in UHV/CVD, according to gas kinetic theory the reactant flux striking the surface is given by

$$Z_{SiH_4} = (N_A/2\pi M_{SiH_4} kT)^{1/2} p_{SiH_4} \quad [cm^{-2}sec^{-1}]$$

where N_A is Avogadro's number, M_{SiH_4} is the molar mass of silane, k is Boltzmann's constant, T the Kelvin temperature, and p_{SiH_4} is the partial pressure of silane. The reaction of silane with the surface requires two active sites [8] and the overall reaction can be written [9]

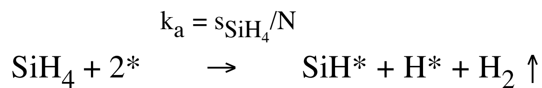

$$SiH_4 + 2* \xrightarrow{k_a = s_{SiH_4}/N} SiH* + H* + H_2 \uparrow$$

where * represents an active site (dangling bond) and X* represents the species X on an active site. The rate constant for the reaction k_a is the ratio of the silane sticking coefficient on a bare surface, designated s_{SiH_4} and the density of surface sites on a bare surface $N = 6.78 \times 10^{14}$ cm^{-2}. As silane cannot react with a hydrogen-terminated site, growth is limited by the desorption of hydrogen from the surface; this is a first-order reaction that may be written

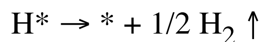

$$H* \rightarrow * + 1/2\ H_2 \uparrow$$

where $k_d = k_{d0} e^{-E_d/kT}$.

Hydrogen desorption from silicon has a number of surprising features and the values of the kinetic parameters have been in some dispute. While there is consensus that desorption is first order in hydrogen coverage and thermally activated, review of the literature [10] shows a range of reported values for E_d and k_{d0}. Lower values of E_d (near 47 kcal/mole) are generally observed on surfaces prepared by growth as compared to those prepared by hydrogen dosing. This has been attributed to a higher step density on surfaces prepared by growth. It can be shown that the vacant site fraction θ in steady state is the solution to

$$0 = -2k_a Z_{SiH_4} \theta^2 + k_d(1-\theta)$$

In the limit of low temperatures, θ is small and the growth rate is limited by hydrogen desorption, so growth is thermally activated and is given by

$$R \approx Nk_d/2 = (N/2)k_{d0}e^{-E_d/kT}$$

and at high temperatures the growth rate is proportional to the silane flux, or

$$R \approx Nk_a Z_{SiH_4} = s_{SiH_4} Z_{SiH_4}$$

Figure 3 shows various measurements of the growth rate from silane in UHV/CVD. The silane sticking coefficent used to fit the data is much less than unity ($s_{SiH_4} \approx 4 \times 10^{-3}$). At low temperatures the growth rate drops exponentially (below about 600 C for the silane pressures used in UHV/CVD). The low value of the silane sticking coefficient leads to high uniformity in UHV/CVD growth because silane molecules scatter from surfaces many times before reacting, leading to nearly uniform fluxes throughout the reactor.

Silicon dioxide surfaces have far fewer dangling bonds, and consequently nucleation on oxidized surfaces is difficult. For short times growth is completely selective [11,12], while at longer times polycrystalline material is formed on silicon dioxide. The maximum selective thickness is enhanced for Ge_xSi_{1-x} layers [13]. The observed maximum selective thicknesses range from a few hundred to about one thousand angstroms. As a result Ge_xSi_{1-x} base regions can be grown selectively and similarly it may be possible to grow elevated source/drain regions with full selectivity. In recent results [13a], small amounts of carbon were found to cause rapid nucleation on silicon dioxide; this phenomenon may be useful when selectivity is *not* desired.

Other reactants

Hydrogen is not incorporated in the growing film but can reduce the growth rate if its partial pressure is sufficiently high. The sticking coefficient of hydrogen on a bare silicon surface is considerably smaller than most reactants of interest ($s_{H_2} \approx 2.5 \times 10^{-5}$ [14,15]. Consequently it is possible to use moderate amounts of hydrogen as a carrier gas or diluent without significantly affecting the growth rates.

Disilane is sometimes used in single-wafer UHV/CVD and GSMBE. Growth from disilane can be modeled well using a sticking coefficient of about 0.04 for temperatures near 600 °C [16]. Although it has been suggested that disilane can react with a hydrogen-terminated surface, recent work has shown the disilane growth rate is limited by hydrogen desorption, similar to silane. Consequently, disilane offers higher growth rates for a given reactant pressure but *only at high temperatures*, while at low temperatures, the growth rate decreases exponentially as for silane. Disilane is particularly advantageous for GSMBE as it results in a decreased gas load for the pumping system at a similar growth rate.

Dichlorosilane is generally not used in UHV/CVD because of persistence of chlorine in the reactor. Growth from dichlorosilane in a single-wafer reactor has been modeled over a wide range of temperatures including low temperatures where the growth rate is limited by surface reactions [17]. Dichlorosilane has a sticking coefficient of about 0.0025 at 577 C [18] and will not react with hydrogen-terminated surfaces. Chemisorption results in both hydrogen and chlorine on the surface. Chlorine desorbs either as $SiCl_2$ or as HCl. Of these competing processes the first results in no net deposition. Consequently growth rates from dichlorosilane are always lower than those from silane or disilane at low temperatures where growth is limited by hydrogen desorption.

Germane is almost universally used as a source of germanium in Ge_xSi_{1-x} heteroepitaxy. By adjusting the partial pressure of germane it is possible to control the germanium concentration in the alloy grown. Similar to silane, chemisorption of germane requires two active sites. Consequently it can be shown [9] that the germanium fraction x is given by

$$1/x = 1 + (M_{GeH_4}/M_{SiH_4})^{1/2}(s_{SiH_4}/s_{GeH_4})(p_{SiH_4}/p_{GeH_4})$$

where $s_{GeH_4} \approx 5.5 \cdot s_{SiH_4}$. Figure 4 shows measured growth rates for Ge_xSi_{1-x} as a function of germanium fraction and temperature. At low temperatures, the growth rate increases with x due to

the increased hydrogen desorption rate from Ge_xSi_{1-x} [19,20]. On the other hand, at high temperatures where the hydrogen coverage is nearly zero the growth rate decreases with x due to the dependence of sticking coefficients on germanium fraction [21]. At intermediate temperatures a peak in the growth rate is observed.

There does not appear to be any obstacle to the growth of Ge_xSi_{1-x} over the entire range of compositions, but most of the reported work concerns silicon-rich ($x < 0.5$) material. Growth of pure germanium by UHV/CVD has been reported [22]. Due to the higher hydrogen desorption rate, germanium layers were grown at temperatures as low as 300-375 °C. In this temperature range the growth rate is thermally activated with $E_A = 33$ kcal/ mole.

Methylsilane (SiH_3CH_3) has been used recently as a carbon source for growth of $Ge_xSi_{1-x-y}C_y$. The sticking coefficient of methylsilane is approximately a factor of a factor of two larger than silane [23]. Methylsilane decreases the growth rate and also appears to increase the efficiency of germanium incorporation [24]. As in other growth techniques, only a small amount of carbon can be incorporated substitutionally; for UHV/CVD growth the maximum substitutional carbon fraction is below 1% [24]. The fraction of substitutional carbon increases with decreasing temperature; good incorporation efficiency together with useful growth rates is obtained at 600 C. For layers with approximately 11% germanium, no degradation of crystal quality is observed with high-resolution X-ray diffraction for carbon concentrations up to about 1% [13a]. However, the fully substitutional carbon concentration is limited to approximately 0.2% in this material. Up to 0.5% fully substitutional carbon can be obtained in silicon layers [13a].

Diborane (B_2H_6) is the only source used for p-type doping. Doping with diborane is very straightforward; diborane requires two active sites with $s_{B_2H_6} \approx 2 \cdot s_{SiH_4}$. Since boron requires the same number of active sites as silane and germane the boron concentration remains nearly the same when germane is introduced [25]. The growth rate is unaffected by diborane until the boron concentration becomes very high [26]. Electrically active boron concentrations as high as 3×10^{20} cm^{-3} have been reported [27]; this is considerably in excess of the equilibrium solid solubility. The lower limit of boron doping is more difficult to determine due to the measurement difficulties. According to SIMS, boron concentrations below the SIMS resolution limit of about 10^{17} cm^{-3} are readily achieved. Smaller concentrations cannot be readily measured by other techniques in the thin layers which are of interest in device applications; however, the actual boron concentrations in these layers may be substantially lower than 10^{17} cm^{-3}.

A boron spike is commonly observed at the initial growth interface with most low-temperature epitaxial growth techniques. This boron spike has a number of causes including atmospheric contamination. Interfacial boron can be controlled by careful control over the wet cleaning process which precedes epitaxy.

Phosphine has been explored for n-type doping. Due to the chemical behavior of n-type dopants on the silicon surface, n-type doping is much more problematic than p-type doping. In the growth of pure silicon, phosphorus is not easily incorporated in the growing layer and consequently it may accumulate on the surface in near-monolayer quantities. Phosphorus forms one fewer bond than silicon and consequently each phosphorus atom on the surface removes one active site from the surface. The overall result is poor phosphorus incorporation *and* a reduced growth rate [28,29]. Phosphorus also accumulates on surfaces and as a result it may be very difficult to grow retrograde profiles. The growth rate of phosphorus-doped silicon is significantly degraded for concentrations greater than the mid-10^{18} cm^{-3} region.

For Ge_xSi_{1-x} growth, n-type doping is somewhat less difficult, with increased incorporation in the growing layer, less seriously degraded growth rates, and more abrupt retrograde profiles [30]. Figure 5 illustrates the results obtained by VLPCVD. In this technique growth takes place at slightly higher pressure, but surface reactions are expected to be dominant and consequently the results should apply to lower pressure techniques such as UHV/CVD. *Arsine* has also been studied and is generally similar in behavior to phosphine [30]. The use of dual deposition chambers may be a solution to the problem of phosphorus persistence, and such an approach may have been used at IBM. However, as noted below, for most applications doping with phosphorus is not a requirement and consequently dopant persistence is not a serious issue.

Transition abruptness

A major objective of low-temperature epitaxial growth is the creation of highly abrupt profiles which cannot be grown with conventional high-temperature epitaxy. Abruptness of transitions can be limited either by fundamental material processes such as surface segregation or the properties of the growth system itself. With the exception of growth using ill-behaved reactants such as phosphine, it is possible to change the gas composition in a UHV/CVD system in a few seconds. At the growth rates typically used ($\approx$ 60 Å/min) this corresponds to profile abruptness on the scale of a monolayer or two.

The profiles are less abrupt than suggested by this estimate due to surface segregation. Both boron and germanium tend to segregate to the growth surface and consequently there is typically a “tail” which occurs upon decreasing either germanium or boron concentrations. The decay length of this tail depends upon growth conditions but under favorable conditions can be of the order of 30 Å/decade [31]. It should be noted that segregation is less severe than in MBE growth at the same temperature due to the presence of hydrogen on the surface [32].

UHV/CVD has been used to grow doped quantum wells tens of angstroms in thickness [33], resonant tunnel diodes [34] and two-dimensional electron gas structures [35] in addition to less aggressive profiles for heterojunction bipolar transistors [36], heterostructure field effect transistors [37], and heterojunction internal photoemission infrared detectors [38]. The first GeSiC-channel heterostructure MOSFETs have been recently fabricated [13a].

Material quality

Much of the reported characterization of UHV/CVD-grown Ge_xSi_{1-x} and $Ge_xSi_{1-x-y}C_y$ material is indirect, using techniques such as photoluminescence, X-ray diffraction, and transmission electron microscopy. In these measurements UHV/CVD material appears to be comparable to that obtained with other techniques. Germanium-silicon epitaxial layers measured by X-ray diffraction are fit perfectly by simulations provided they are grown below the equilibrium critical thickness.

There are a smaller number of reports of electrical characterization of UHV/CVD grown material. Nguyen et al. report minority carrier lifetime as high as 160 μs [39] in multiwafer UHV/CVD. Lifetime as high as 400 μs has been reported by Sanganeria et al. [40] who used a single-wafer, cold-wall reactor. The low-temperature electron mobility in modulation-doped structures is as high as 5.2×10^5 $cm^2/V{\cdot}sec$. Of course, the ultimate test of a material is in an application; in this respect, UHV/CVD has been used to fabricate heterojunction bipolar transistors of very high performance [36]. Other recent results include the observation of enhanced mobility over silicon for $Ge_xSi_{1-x-y}C_y$ heterostructure field effect transistors [13a].

A possible liability of the UHV/CVD technique is the difficulty of growing abrupt retrograde phosphorus profiles in silicon. This is balanced by the advantages of a multiwafer technique, and the beneficial effects of hydrogen in reducing surface segregation and surface mobility during growth.

Process integration and device structures

As noted earlier, one of the limitations of the UHV/CVD technique is the difficulty of growing heavily n-type layers. This has not been a significant obstacle to process integration, however. The major present application for UHV/CVD is for heterojunction bipolar transistors. State-of-the-art HBTs need to be self-aligned structures, and this is facilitated by the use of a polysilicon emitter. In the polysilicon emitter process, a p-type base region is formed typically followed by deposition of undoped polysilicon which is subsequently ion-implanted. An ion implant anneal follows which causes rapid diffusion through the polysilicon and emitter formation in the epitaxial layer. Such a structure does not require n-type epitaxial layers and is actually preferred over a single-crystal emitter as lower minority carrier diffusivity in polysilicon leads to higher emitter injection efficiency.

Successful process integration with APCVD or RPCVD also has limitations, albeit different ones. Generally a high-temperature clean is performed before epitaxy begins which leads to a higher thermal budget. Completely selective growth is possible (due to the use of chlorine-containing reactants) but at the same time there is often pattern dependence of growth rates and germanium fraction.

CVD at higher pressures (LPCVD, RTCVD, LRP, RPCVD, and APCVD)

A considerable body of research has explored low-temperature CVD growth at higher total pressures, ranging from just above the 10^{-3} Torr range characteristic of UHV/CVD to atmospheric pressure. In this section, we briefly summarize the characteristics of these related growth techniques. These reactors operate at higher pressures than UHV/CVD and consequently it is possible that there will be significant gas-phase chemistry, depending upon the growth temperature and residence time. Gas phase reactions may increase the growth rate due to the formation of highly reactive intermediates and may also alter the dopant incorporation process. On the other hand, higher pressure may permit the formation of a stagnant boundary layer which reduces reactant transport to the surface, tending to decrease the growth rate.

Many systems also use chlorine-containing reactants and/or hydrogen carrier gas. Generally speaking, the available deposition rates from chlorine-containing reactants are less than those from silane at the same temperature. Hydrogen carrier gas may have no effect on the growth rate (at low

partial pressures) or may result in a decrease in growth rate. The discussion below is ordered roughly according to increasing total pressure.

Hot-wall *low-pressure chemical vapor deposition* (LPCVD) of silicon and Ge_xSi_{1-x} with a total pressure of 0.30 Torr and with hydride reactant partial pressures of 50 mTorr and above has been reported by Lee et al. [41]. High phosphorus dopant concentrations ($\approx 10^{20}$ cm^{-3}) were observed along with little depression in growth rate; this could be a consequence of gas phase reactions leading to the formation of highly reactive intermediates not found in UHV/CVD. Vescan et al. have studied growth by cold-wall LPCVD at a pressure near 100 mTorr although with dichlorosilane source gas [42]; use of chlorine-containing reactants is particularly advantageous in achieving selective growth [43]. In this case, gas phase reactions were probably also present, as evidenced by the applicability of equilibrium thermochemistry [43]. However, it appears that surface reactions may dominate even at higher pressures provided the residence time is small enough. For example, Dutartre and coworkers [44] studied silicon growth at 0.03 Torr partial pressure of silane and a hydrogen carrier gas to give a total pressure of 1.5 Torr. The growth rates could be modeled well using the same surface-reaction based model described above provided the effect of the hydrogen carrier gas was included. As noted earlier, in modeling studies the transition from surface reaction rate-dominated to gas phase reaction-dominated can be also seen; in the particular case investigated in one modeling study gas phase reactions became important above 800 °C [17]. (Of course, the temperature at which gas phase reactions become important can be expected to depend greatly on reactor design). Considerable research has been performed by two groups using single-wafer reactors with total pressures near 6 Torr (hydrogen carrier gas) and 0.05 Torr (dichlorosilane reactant). The technique has been termed *limited reaction processing* (LRP) [45] or *rapid thermal chemical vapor deposition* (RTCVD) [46] depending upon whether temperature excursions or rapid gas switching (respectively) are used to make compositional changes. The high-pressure limit is represented by conventional silicon epitaxy, which is either at atmospheric pressure [47,48] or possibly slightly below atmospheric pressure, typically at 76 Torr. Modern reactors of this type are single-wafer reactors and were designed for conventional epitaxy at temperatures near 1100 °C. Hydrodynamic boundary layer effects and gas phase reactions are both very important in these reactors. APCVD reactors have particular advantages with respect to phosphorus doping [49] and selective growth [50].

Most, although not all, of the reactors operating at higher pressures are single-wafer reactors. This leads to concern about wafer throughput when used to grow layers at low temperatures, where growth rates may be limited by hydrogen desorption kinetics. Process development can also be

more difficult; as material composition and doping is determined by a complex interplay between gas phase chemistry and surface reaction kinetics.

An important emerging application for UHV/CVD and other techniques is the growth of germanium-silicon-carbon layers. Small amounts of carbon ($\approx 0.2\%$) considerably improve the thermal stability of strained epitaxial layers. As a result, it becomes possible to increase the germanium fraction or thickness above that possible for ordinary germanium-silicon material. These materials are expected to have important applications for heterostructure field effect transistors and heterojunction bipolar transistors.

References

1. B.S. Meyerson, *Appl. Phys. Lett.* **48**, 797-799 (1986).
2. B.S. Meyerson, U.S. Patent 5,298,452.
3. A.J. Pidduck, D.J. Robbins, A.G. Cullis, W.Y. Leong, and A.M. Pitt, *Thin Solid Films* **222**, 78-84 (1992).
4. K.E. Violette, M.K. Sanganeria, M.C. Özturk, G. Harris, and D.M. Maher, *J. Electrochem. Soc.* **141**, 3269 (1994).
5. F. Glowacki and Y. Campidelli, *Microelectron. Eng.* **25**, 161-70 (1994).
6. F. Sato, T. Taksumi, T. Hashimoto, and T. Tashiro, *IEEE Trans.* **ED-41**, 1373 (1994).
7. B.S. Meyerson, F.J. Himpsel, and K.J. Uram, *Appl. Phys. Lett.* **57**, 1034-1036 (1990).
8. S.M. Gates, C.M. Greenlief, and D.B. Beach, *J. Chem. Phys.* **93**, 7493-7503 (1990) and references therein.
9. D.W. Greve, in *Thin Films: Advances in Research and Development*, Volume 23, M.H. Francombe and J.L. Vossen, eds., Academic Press, 1998.
10. D.J. Doren, in *Advances in Chem. Phys.,* Vol. XCV, I. Prigogine and S.A. Rice, eds., J. Wiley and Sons, 1996.
11. H. Hirayama, T. Tatsumi, A. Ogura, and N. Aizaki, *Appl. Phys. Lett.* **51** 2213-15, (1987).
12. T-R. Yew and R. Reif, *J. Appl. Phys.* **65**, 2500-7 (1989).
13. M. Racanelli and D.W. Greve, *Appl. Phys. Lett.* **58**, 2096 (1991).

13a. A. Mocuta, Ph.D. thesis (Carnegie Mellon University, 1999).

14. D. Dutartre, P. Warren, I. Berbezier, and P. Perret, *Thin Solid Films* **222**, 52-56 (1992).
15. D.J. Robbins, J.L. Glasper, A.G. Cullis, and W.Y. Leong, *J. Appl. Phys.* **69**, 3729-3732 (1991).
16. X.F. Hu, Z. Xu, D. Lim, M.C. Downer, P.S. Parkinson, B. Gong, G. Hess, and J.G. Ekerdt, *Appl. Phys. Lett.* **71**, 1376 (1997) and references therein.
17. M. Hierlemann, A. Kersch, C. Werner, and H. Schäfer, *J. Electrochem. Soc.* **142**, 259- 266 (1995).
18. P.A. Coon, P. Gupta, M.L. Wise, and S.M. George, *J. Vac. Sci. Technol.* **A10**, 324-333 (1992)].
19. B.M.H. Ning and J.E. Crowell, *Appl. Phys. Lett.* **60**, 2914-2916 (1992).
20. B.M.H. Ning, C.R. Crowell, *Surf. Sci.* **295**, 79-98 (1993) look for more recent.
21. D.J. Robbins, J.L. Glasper, A.G. Cullis, and W.Y. Leong, *J. Appl. Phys.* **69**, 3729- 3732 (1991).
22. B. Cunningham, J.O. Chu, and S. Akbar, *Appl. Phys. Lett.* **59**, 3574 (1991).

23. A.C. Mocuta and D.W. Greve, (to appear in Proc. MRS Spring Meeting, San Francisco, CA, April, 1998).
24. A.C. Mocuta and D.W. Greve (to be published).
25. D.W. Greve and M. Racanelli, *J. Electron. Mater.* **21**, 593 (1992).
26. D.W. Greve, R. Misra, R. Strong, and T.E. Schlesinger, *J. Vac. Sci. Technol.* **A12**, 979 (1994).
27. R. Strong, R. Misra, D.W. Greve, and P.C. Zalm, *Journal of Applied Physics* **82**, 5191 (1997).
28. D.W. Greve and M. Racanelli, *J. Electrochem. Soc.* **138**, 1744 (1991).
29. M.L. Yu, D.J. Vitkavage, and B.S. Meyerson, *J. Appl. Phys.* **59**, 4032 (1986).
30. S-M. Jang, K. Liao, and R. Reif, *J. Electrochem. Soc.* **142**, 3520 (1995).
31. R. Strong, R. Misra, D.W. Greve, and P.C. Zalm, *Journal of Applied Physics* **82**, 5191 (1997).
32. D.A. Grützmacher, T.O. Sedgwick, A. Powell, M. Tejwani, S.S. Iyer, J. Cotte, and F. Cardone, *Appl. Phys. Lett.* **63**, 2531-2533 (1993).
33. R. Misra, D.W. Greve, and T.E. Schlesinger, *Appl. Phys. Lett.* **67**, 2548 (1995).
34. K. Ismail, B.S. Meyerson, and P.J. Wang, *Appl. Phys. Lett.* **59**, 973 (1991).
35. P.J. Wang, F.F. Fang, B.S. Meyerson, J. Nocera, and B. Parker, *Appl. Phys. Lett.* **54**, 2701 (1989).
36. G.L. Patton, J.H. Comfort, B.S. Meyerson, E.F. Crabbé, G.J. Scilla, E. de Frésart, J.M.C. Stork, J.Y.-C. Sun, D.L. Harame, and J.N. Burghartz, *IEEE Electron Device Letters* **EDL-11**, 171-173 (1990).
37. K. Ismail, B.S. Meyerson, S. Rishton, J. Chu, S. Nelson, and J. Nocera, *IEEE Electron Dev. Lett.* **EDL-13**, 229 (1992).
38. R. Strong, D.W. Greve, P. Pellegrini, and M. Weeks, *Journal of Applied Physics* **82**, 5199 (1997).
39. T.N. Nguyen, D.L. Harame, J.M.C. Stork, F.K. LeGoues, and B.S. Meyerson, IEDM 1986 pp. 304-7.
40. M.K. Sanganeria, K.E. Violette, and C. Özturk, *Appl. Phys. Lett.* **63**, 1225 (1993).
41. C.-J. Lee, M. Sakuraba, M. Ishiii, T. Matsuura, J. Murota, I. Kawashima, and N. Yabumoto, *Electrochem. Soc. Proc.* **97-25**, 1356-1363 (1997).
42. L. Vescan, H. Beneking, and O. Meyer, *J. Cryst. Growth* **76**, 63 (1986).
43. L. Vescan, *Mat. Sci. and Engrg.* **B28**, 1-8 (1994).
44. D. Dutartre, P. Warren, I. Berbezier, and P. Perret, *Thin Solid Films* **222**, 52- 56 (1992).
45. J.L. Hoyt, C.A. King, D.B. Noble, C.M. Gronet, J.F. Gibbons, M.P. Scott, S.S.

Laderman, S.J. Rosner, K. Nauka, J. Turner, and T.I. Kamins, *Thin Solid Films* **184**, 93 (1990).

46. P.M. Garone, J.C. Sturm, P.V. Schwartz, S.A. Schwarz, and B.J. Wilkens, *Appl. Phys. Lett.* **56**, 1275 (1990).
47. T.K. Kamins and D.J. Meyer, *Appl. Phys. Lett.* **61**, 90 (1992).
48. P.D. Agnello, T.O. Sedgwick, M.S. Goorsky, J. Ott, T.S. Kuan, and G. Scilla, *Appl. Phys. Lett.* **59**, 1479-1481 (1991).
49. P.D. Agnello, T.O. Sedgwick, and J. Cotte, *J. Electrochem. Soc.* **140**, 2703-2709 (1993).
50. T.O. Sedgwick, D.A. Grützmacher, A. Zaslavsky, and V.P. Kesan, *J. Vac. Sci. Technol.* **B 11**, 1124-1128 (1993).

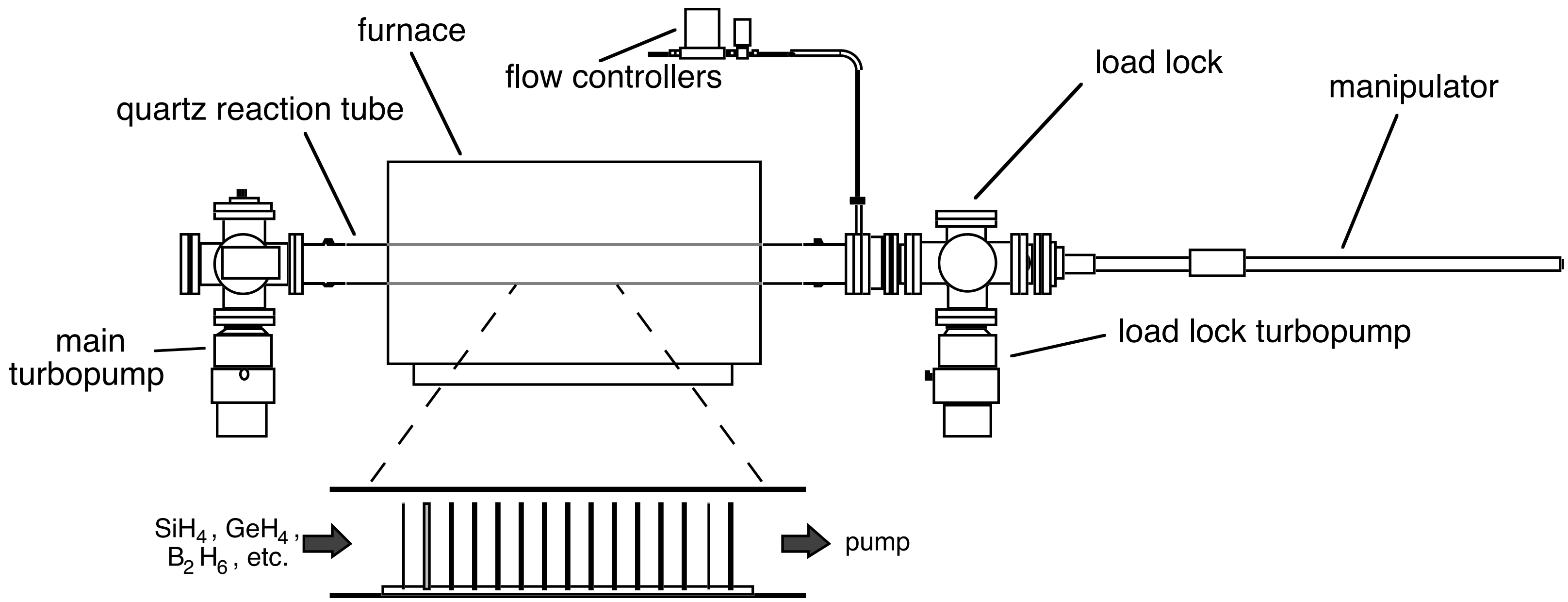

Figure 1. Schematic diagram of UHV/CVD growth system.

Return

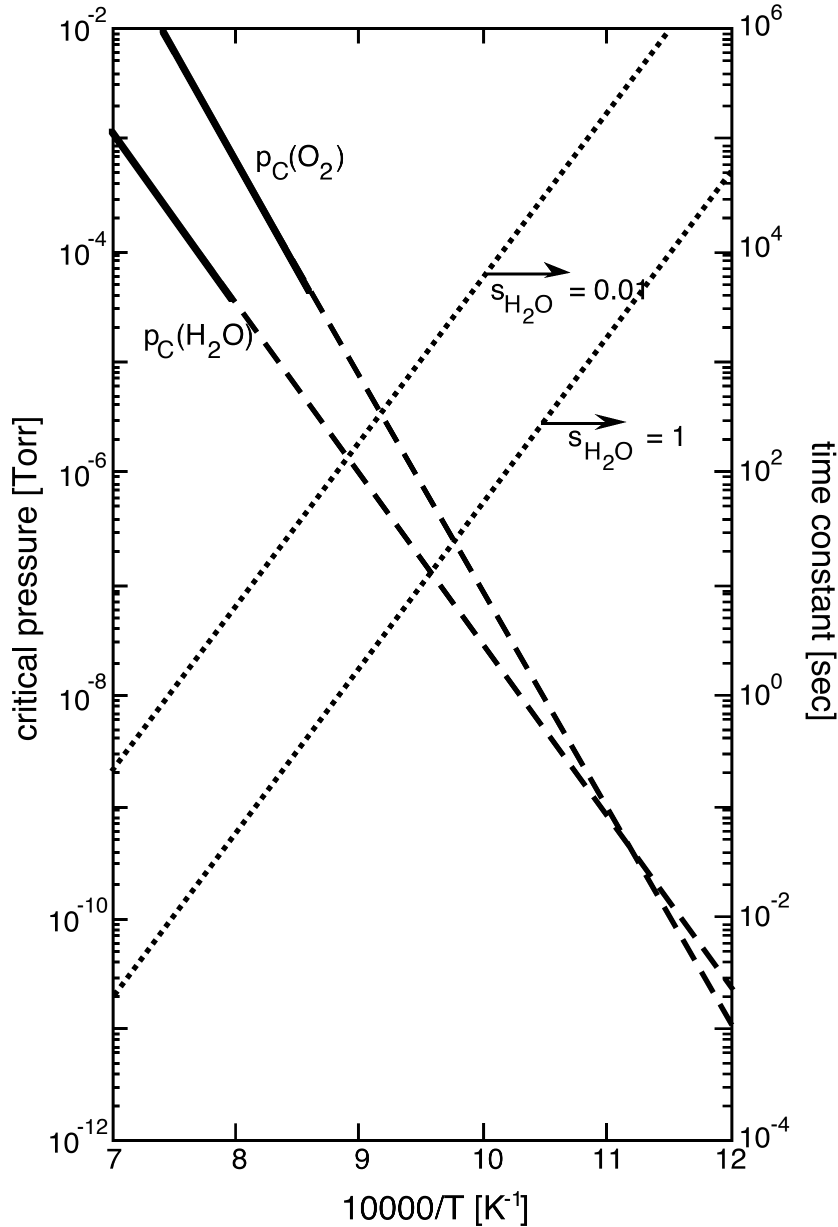

Return

Figure 2. Conditions for achieving and maintaining an oxygen-free surface for epitaxial layer growth. The left axis indicates the critical water vapor and oxygen partial pressures to obtain a surface half covered with oxygen in equilbrium. (Critical pressure data from [F.W. Smith and G. Ghidini, *J. Electrochem. Soc.* **129** (1982)] and [G. Ghidini and F.W. Smith, *J. Electrochem. Soc.* **131**, 2924-2928 (1984)]. Partial pressures below this critical value will result in a nearly oxygen-free surface. The solid lines indicate the temperature range in which the data was acquired. The right axis shows the estimated time constant for oxygen desorption. The time constant depends on the value assumed for the water vapor sticking coefficient. *Return*

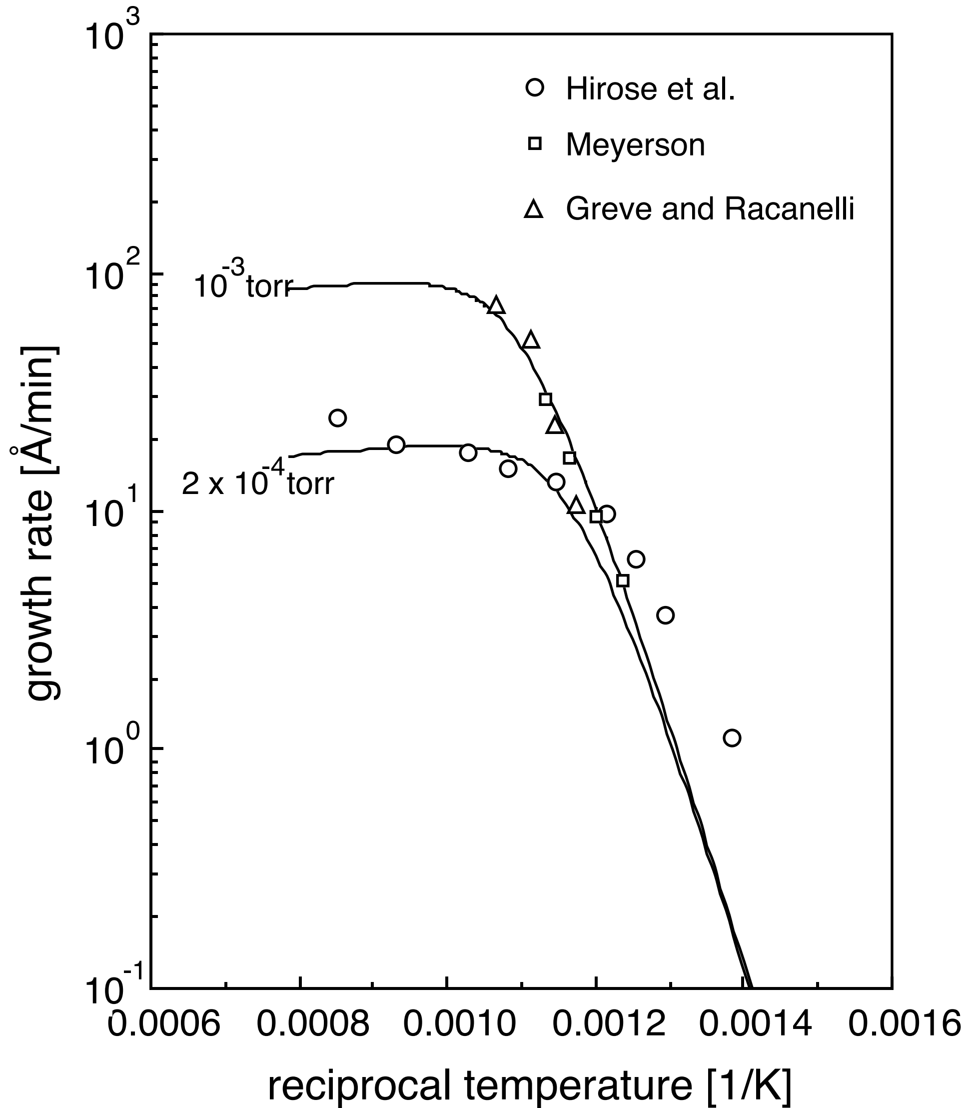

Return

Fig. 3. UHV/CVD growth rates. Data from Meyerson [data derived from S.K. Kulkarni, S.M. Gates, B.A. Scott, and H. Sawin, *Surf. Sci.* **239**, 13- 24 (1990)]; [D.W. Greve and M. Racanelli, *J. Electrochem. Soc.* **138**, 1744 (1991)]; and [F. Hirose, M. Suemitsu, and N. Miyamoto, *Japan. J. Appl. Phys.* **29**, L1881 (1990)].

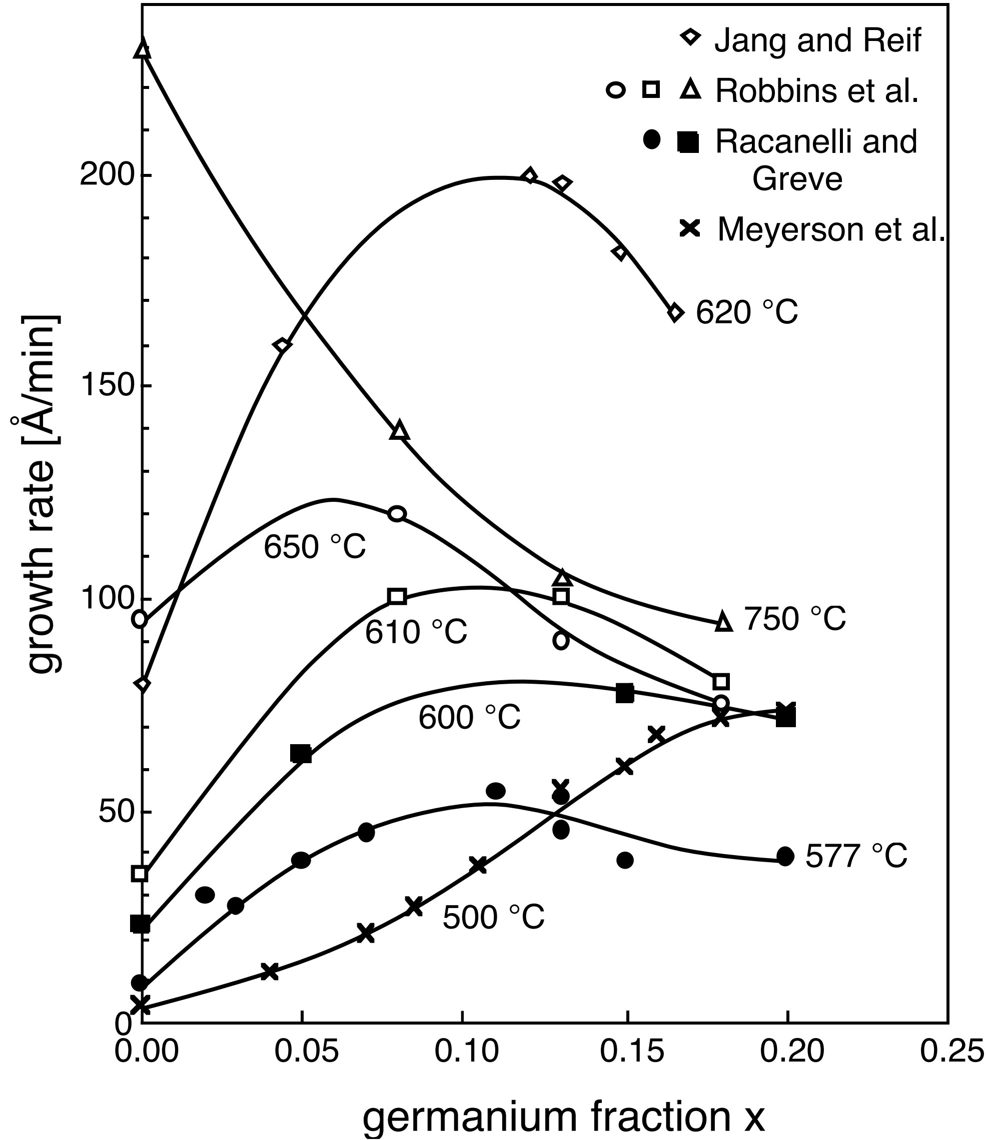

Return

Figure 4. Growth rate of Ge_xSi_{1-x} as a function of temperature. At low temperatures growth is limited by hydrogen desorption, which becomes more rapid as the germanium fraction increases; while at high temperatures the surface is hydrogen-free, and the behavior of the sticking coefficient with germanium fraction dominates. For intermediate growth temperatures a peak in the growth rate as a function of germanium fraction is observed. Data from B.S. Meyerson, K.J. Uram, and F.K. LeGoues, *Appl. Phys. Lett.* **53**, 2555 (1988); M. Racanelli and D.W. Greve, *Appl. Phys. Lett.* **56**, 2524 (1990); D.J. Robbins, J.L. Glasper, A.G. Cullis, and W.Y. Leong, *J. Appl. Phys.* **69**, 3729 (1991); S.-M. Jang and R. Reif, *Appl. Phys. Lett.* **59**, 3162-3124 (1991)]. Data of Robbins et al. and Reif et al. are for silane partial pressures of about 5 mTorr.

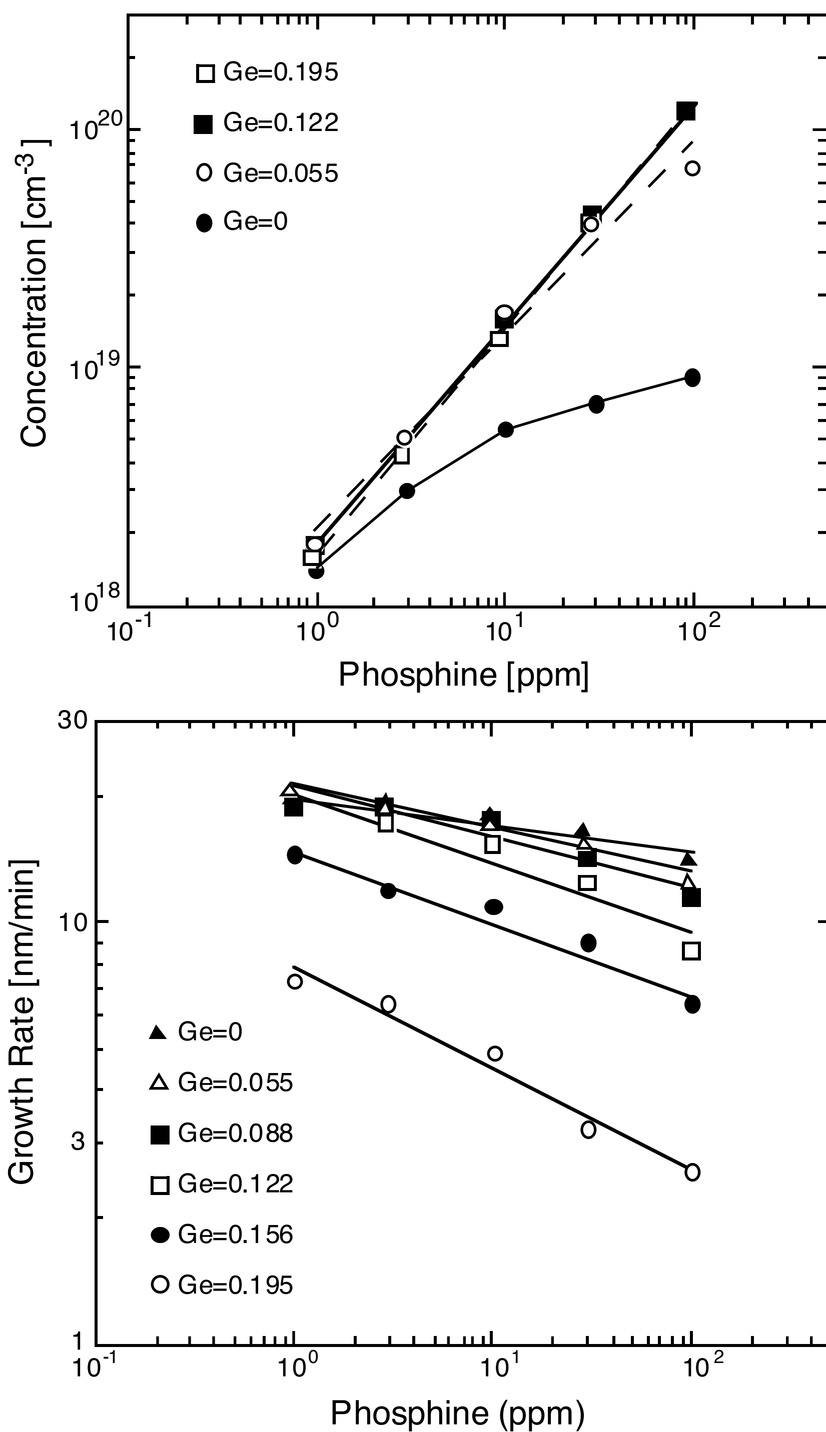

Return

Fig. 5. Phosphorus incorporation during growth from silane and germane at 620 °C with a total pressure of about 7 mTorr: (a) phosphorus concentration as a function of phosphine concentration and (b) growth rate as a function of phosphorus concentration. [Figures 7 and 9 from S-M. Jang, K. Liao, and R. Reif, *J. Electrochem. Soc.* **142**, 3520 (1995)] Similar results are expected during UHV/CVD growth at lower pressures.